Nuclear Technology

ISSN: 0029-5450 (Print) 1943-7471 (Online) Journal homepage: http://www.tandfonline.com/loi/unct20

Iodine Atom Diffusion in SiC and Zirconium with First-Principles Calculations

Ruixuan Han, Liucheng Liu, Rui Tu, Wei Xiao, Yingying Li, Huailin Li & Dan Shao

To cite this article: Ruixuan Han, Liucheng Liu, Rui Tu, Wei Xiao, Yingying Li, Huailin Li & Dan Shao (2016) Iodine Atom Diffusion in SiC and Zirconium with First-Principles Calculations, Nuclear Technology, 195:2, 192-203, DOI: 10.13182/NT15-109

To link to this article: http://dx.doi.org/10.13182/NT15-109

Published online: 27 Mar 2017.

ANS

NUCLEAR TECHNOLOGY · VOLUME 195 · 192–203 · AUGUST 2016

Iodine Atom Diffusion in SiC and Zirconium with First-Principles Calculations

Ruixuan Han,[a,b] Liucheng Liu,[c] Rui Tu,[d] Wei Xiao,[a,b]* Yingying Li,[a,b] Huailin Li,[a,b] and Dan Shao[c]

[a]*State Nuclear Power Research Institute, Division of Nuclear Materials and Fuel, Beijing 100029, China*
[b]*National Energy R&D Center of Nuclear Grade Zirconium Materials, Beijing 100029, China*
[c]*Jianghan University, School of Physics and Information Engineering, Wuhan 430056, China*
[d]*Wuhan University, School of Physics and Technology, Wuhan 430072, China*

Received August 12, 2015
Accepted for Publication January 26, 2016
http://dx.doi.org/10.13182/NT15-109

Abstract — *Iodine atom interstitial configurations and diffusion in bulk β-SiC and α-Zr are calculated using first-principles calculations and the nudged elastic band method. The formation energy of an I interstitial in bulk silicon carbide (SiC) is ten times higher than that of an I interstitial in bulk Zr. The I interstitial is very difficult to introduce into bulk SiC compared with the doping process in bulk Zr. The diffusion mechanisms of an I atom in SiC and Zr are exchange mechanisms. Iodine interstitial diffusion in bulk SiC is roughly an isotropic process along a path that is a series of combinations of* $I_{Si} \rightarrow I_c$ *and* $I_c \rightarrow I_{Si}$*, with a diffusion barrier of 1.20 eV and an attempt-to-diffuse frequency* $\Gamma_0 = 25.12$ *THz. Meanwhile, I interstitial diffusion in bulk Zr is an anisotropic process. An I interstitial atom diffuses mainly between two Zr atom [0001] layers along a zigzag path with a diffusion barrier of 0.16 eV and an attempt-to-diffuse frequency* $\Gamma_0 = 2.88$ *THz. In general, the diffusion rate of an I interstitial in bulk SiC is lower than that in bulk Zr in the temperature range from 290 to 3000 K. The defect effect on I diffusion is an interesting topic for future study.*

Keywords — *Diffusion, iodine, cladding materials.*

Note — *Some figures may be in color only in the electronic version.*

I. INTRODUCTION

The fuel cladding is an important safety barrier in fission nuclear reactors because it restrains most of the radioactive fission products within its volume.[1] Understanding the mechanisms of fission product diffusion in the fuel cladding materials is of great interest.[2] Although zirconium is currently the most used fuel cladding material,[3] silicon carbide (SiC) is a promising light water reactor cladding material because of its high-temperature fission gas retention, high corrosion resistance, good thermal conductivity, and low neutron absorption cross section.[4–8] The ability to keep radioactive fission products within the cladding material determines whether SiC can be used as a safe cladding material.

Radioactive iodine isotopes, especially ^{129}I ($T_{1/2}$ = 15.7×10^6 years) and ^{131}I ($T_{1/2}$ = 8 days), are important fission products and of radioecological relevance because of their accumulation in the thyroid gland with a biological half-life of ~140 days (Ref. 9). In addition, they may cause the iodine-induced stress corrosion cracking that occurs on the inner wall of the Zr fuel cladding.[10–12]

Ion implantation of iodine into Zr (Ref. 13) and SiC (Refs. 9, 14, and 15) have been carried out to study I diffusion properties in cladding materials. Especially, the Arrhenius diagram, diffusion coefficients, and activation energy of I diffusion in Zr have been reported.[13] However, diffusion of iodine in SiC is not clear, and few experimental and simulation data have been reported.[2,14,15]

*E-mail: xiaowei@snptc.com.cn

First-principles calculation is a feasible method to study the diffusion mechanism, which could overcome limitations of the experimental study, such as radioactivity, detection limitation, expensive cost, etc. Iodine diffusion in zirconium has been studied with computational simulations,[16–18] including the diffusion of iodine on exposed metal surfaces and/or crack faces[16,17] and the diffusion of iodine in bulk Zr (Ref. 18). Diffusion of other elements in SiC have also been reported.[19–21]

In this paper, first-principles calculations and the nudged elastic band (NEB) method are carried out to study the I interstitial in bulk SiC and Zr. The diffusion rates as a function of temperature of I interstitial atom diffusion in bulk SiC and Zr are calculated. The results show that the diffusion rate of an I atom in bulk SiC is much lower than that in bulk Zr.

II. CALCULATION METHODS AND MODELS

II.A. Calculation Methods

Density functional theory calculations[16,22] are performed to calculate the ground state energies of the systems, and the energy calculations are performed with the Vienna ab initio Simulation Package (VASP) code.[5,23,24] The projected augmented wave method[25,26] is used to deal with the wave functions near the core region. The exchange correlation functional within the generalized gradient approximation parameterized by Perdew, Burke, and Ernzerhof[27,28] (PBE) is used in the calculations. For calculations with more than one species, the maximum cutoff value is used for the calculation. As a result, the cutoff of the plane-wave kinetic energy for the SiC + I system is 400 eV since the ENMAX of C is the highest and it is 400 eV; the cutoff of the Zr + I system is 176 eV because the ENMAX of I is 176 eV, which is higher than that of Zr. For a 65-atom SiC + I system, the system energy difference between the calculation with a 2×2×2 Monkhorst Pack *k*-point mesh and the calculation with a 4×4×4 *k*-point mesh is <0.01%. In the energy calculations for structure relaxation, diffusion path search, and frequency modes, the summations over the Brillouin zone are performed with a 2×2×2 Monkhorst Pack *k*-point mesh. In the electronic relaxation calculation, the residual minimization method with direct inversion in the iterative subspace[29,30] is used, and the energy convergence criterion is 10^{-4} eV. The conjugate gradient method is used to minimize the Hellmann-Feynman forces in the ionic relaxations with the force stopping criterion of 0.05 eV/Å. Spin polarization is used in all calculations.

The climb image NEB method[31–33] is used to search the minimal energy paths and the saddle points of I interstitial diffusion in bulk SiC and Zr. The VTST code[34] combined with VASP is performed in the diffusion calculations. The quick-min method is used to relax the NEB forces. In most of the NEB calculations, there are four images between the initial and final configurations. In some cases, eight images are used. The spring constant of the NEB calculations is 5.0 eV/Å^2, and the force convergence criterion is 0.05 eV/Å. In the NEB calculations, the volume is fixed. Although a single interstitial atom may generate local pressure around the defect, the system volume may not change too much during the single-atom diffusion process, especially for a large supercell.

For an I interstitial atom in bulk SiC or Zr, the interstitial formation energy ΔE_i^f is defined as

$$\Delta E_i^f = E_i - E_{\mathrm{I}} - E_{Pure}\,, \tag{1}$$

where

E_{Pure} = total energy of a SiC or Zr supercell without any I atom

E_i = total energy of a SiC or Zr supercell with an I interstitial atom

E_{I} = ground state energy of a single iodine atom calculated in the empty box used for the SiC or Zr supercell.

II.B. Calculation Models

Known as carborundum, β-SiC has a zincblende crystal structure (similar to diamond). Each atom connects four nearest-neighbor atoms of other species by covalent bonds. A 2×2×2 β-SiC supercell with 64 atoms is used to simulate the diffusion process. Its structure is shown in Fig. 1a.

Hexagonal close packed (hcp) α-Zr is composed of hexagonal atom layers as the ABAB . . . sequence along the [0001] direction (see Figs. 1b and 1c). The supercell used to simulate the I diffusion process in α-Zr has 2×2×2 Zr primary cells with 64 atoms. The SiC and Zr supercells are big enough to eliminate the interaction between the I interstitials inside neighboring unit cells due to the periodic boundary condition.

III. RESULTS AND DISCUSSION

III.A. Iodine Interstitial Diffusion in Bulk SiC

III.A.1. Configurations of an I Interstitial Atom in Bulk SiC

With the PBE pseudopotential, our optimized lattice parameter of SiC is a = 4.37 Å. It agrees well with the

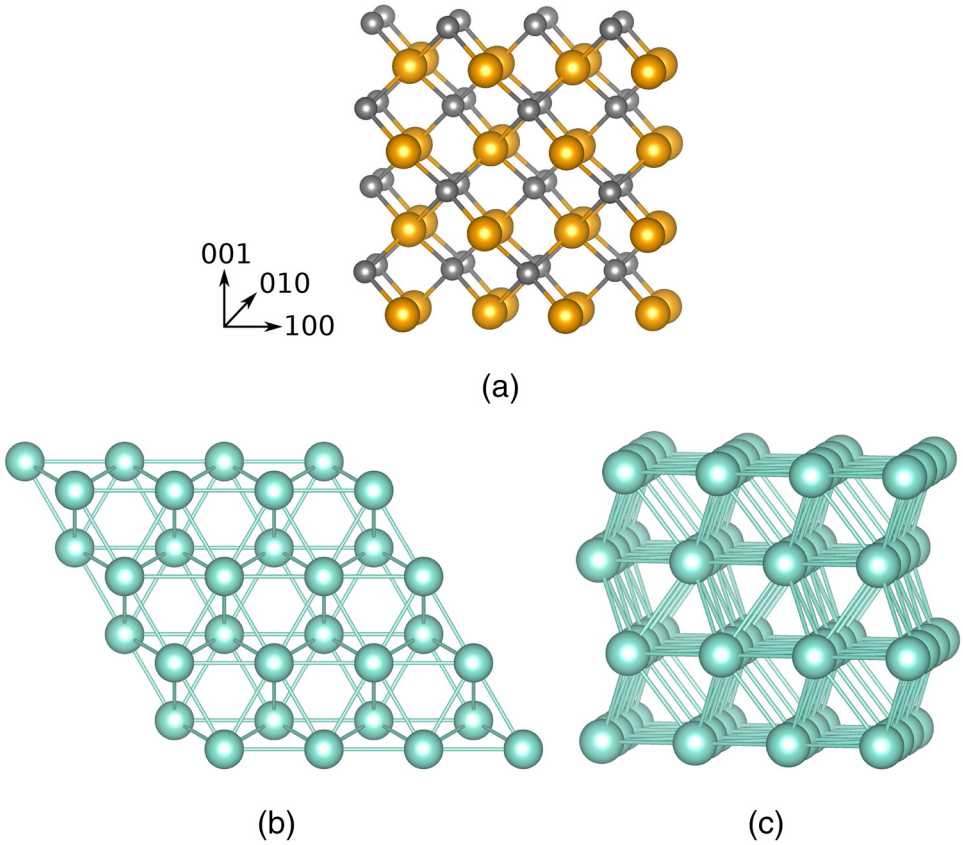

Fig. 1. The supercells of β-SiC and α-Zr used in the calculations. (a) β-SiC supercell, where the larger balls represent Si atoms and the smaller ones are C atoms; (b) top view of α-Zr supercell and (c) side view of α-Zr supercell, where in (b) and (c), all balls are Zr atoms. Both supercells contain 64 atoms.

experimental data (a = 4.3596 Å) (Ref. 35). Three possible configurations of an I interstitial in bulk SiC are shown in Fig. 2. In configuration type 1 (Fig. 2a), the I interstitial occupies the lattice of a Si atom, and the Si atom is squeezed into a neighbor octahedral site as an interstitial atom. In configuration type 2 (Fig. 2b), the I atom occupies the lattice of a carbon atom, and the carbon atom is squeezed into a neighbor octahedral site as an interstitial atom. In configuration type 3 (Fig. 2c), the I atom locates in an octahedral site. The formation energies of the three types of interstitial configuration in the 64 + 1 atom supercell are 14.41, 15.40, and 19.42 eV separately. This suggests that interstitial configuration type 1 is the most stable one.

III.A.2. Diffusion Path of I Atom Diffusion in Bulk SiC

Since the configuration of an I atom located at a Si lattice is the most stable, an I interstitial may migrate from a Si lattice to another adjacent Si lattice site. Ignoring the influence of the squeezed Si atom, all of the other Si atoms in the SiC bulk are equivalent. The I interstitial atom may diffuse along multiple Si-Si edges.

A schematic of I interstitial diffusion multiple step paths and the corresponding system energies are shown in Fig. 3. In Fig. 3, an I interstitial diffuses from a Si lattice site to one of the nearest Si sites. A metastable state appears in the energy plot. Actually, the configuration of the metastable state is the configuration of type 2 in Fig. 2b. This suggests that the iodine diffusion between two neighboring Si atoms can decompose into two steps. In the first step, the I interstitial diffuses from a Si site (type 1) to an adjacent C site (type 2). In the second step, the I interstitial atom diffuses from a C site to another adjacent Si site. In the first step, the energy barrier ($I_{Si} \rightarrow I_c$) is 1.20 eV, and the reverse barrier is 0.09 eV. In the second step, the energy barrier for $I_c \rightarrow I_{Si}$ is 0.19 eV, and the reverse barrier is 1.27 eV. Therefore, the first step of the diffusion is the control step, and the diffusion barrier of an I atom migrating from a Si site to a neighboring Si site in bulk SiC is 1.20 eV.

When an I interstitial atom occupies a Si or C lattice, the Si or C atom will be squeezed into a neighboring octahedral site. As a result, the symmetry of the SiC structure is broken (see Fig. 4). In Fig. 4a, the diffusion of

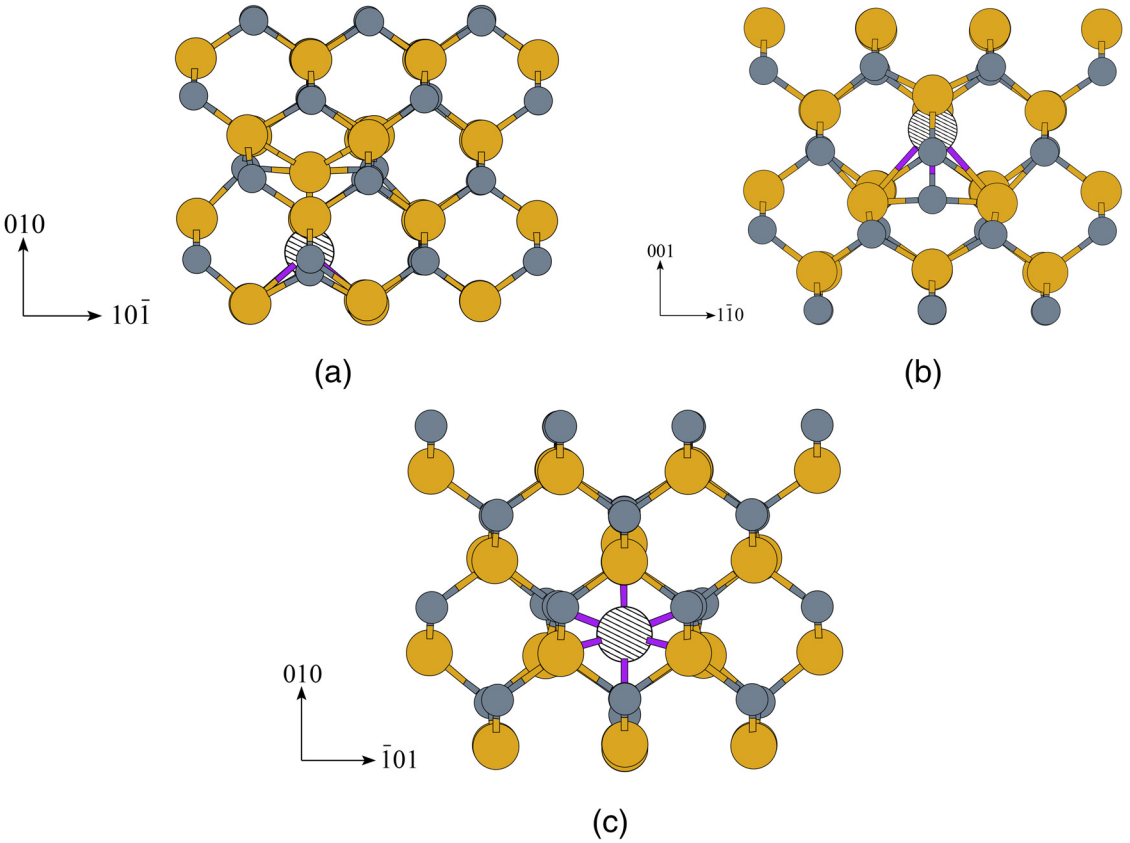

Fig. 2. Three possible configurations for an I interstitial atom in bulk SiC. The big balls represent Si atoms, the small ones are C atoms, and the patterned one is the I interstitial. (a) Type 1: An I interstitial takes the position of a Si atom, and the Si atom is squeezed into an octahedral site. (b) Type 2: An I interstitial takes the position of a C atom, and the C atom is squeezed into an octahedral site. (c) Type 3: An I interstitial is in an octahedral site.

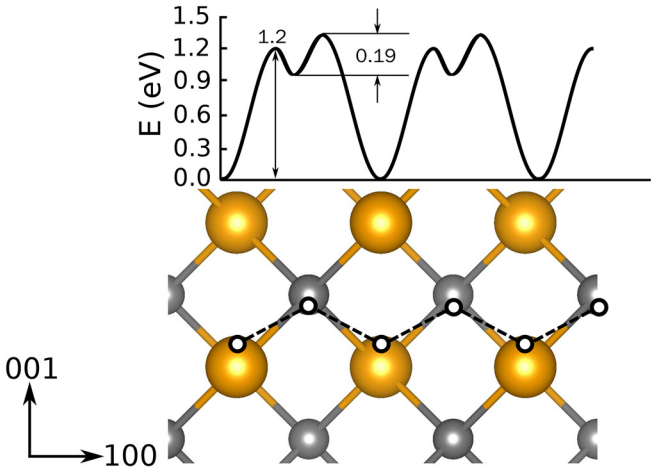

Fig. 3. Energy profile and schematic of a corresponding possible diffusion path for iodine atom diffusion in SiC bulk. An I interstitial diffuses from a Si site to a neighbor C site and then to another Si neighbor site. The larger balls represent Si atoms, and the smaller ones are C atoms. The black unfilled circles with dashed lines represent the metastable configuration positions of an iodine atom in SiC bulk and a possible diffusion path.

an I interstitial from a Si site to a neighbor C site may be via two different paths: paths A and B. Since the symmetry is broken, the distance between the I interstitial and the adjacent carbon atom along path A is L_A = 2.11 Å, while the distance between the I atom and the adjacent carbon atom along path B is L_B = 2.79 Å. Path B is close to the interstitial Si atom at the octahedral site. The diffusion energy barriers for the two possible paths in Fig. 4a are listed in Table I. The diffusion barrier for path A is E_A = 1.20 eV. Diffusion path B can be decomposed into two steps; the barrier for the first step is E_{B1} = 0.88 eV, and it is E_{B2} = 1.20 eV for the second step. A higher barrier makes the second step the control step along path B. Therefore, the diffusion barriers for paths A and B are close.

Similarly, an I interstitial atom can migrate from a C site to a neighbor Si site via two different paths: paths C and D (see Fig. 4b). The diffusion length of path C is L_C = 2.36 Å, while the length of path D is L_D = 2.67 Å. Diffusion path D is closer to the carbon atom at the interstitial sites. The diffusion energy barriers of the two paths are listed in Table I. The diffusion barrier for path C

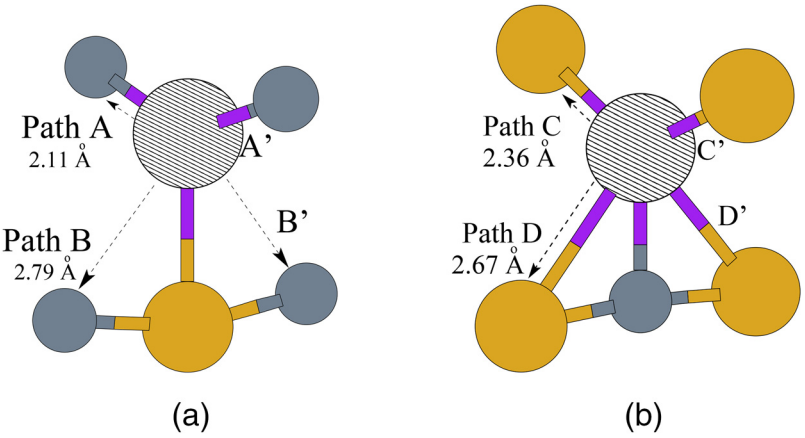

Fig. 4. The diffusion paths of an I interstitial atom diffuse from a lattice of Si or C atom to an adjacent site. (a) Iodine diffusion from $I_{Si} \rightarrow I_c$ and (b) I diffusion from $I_c \rightarrow I_{Si}$. The big balls represent Si atoms, the small ones are C atoms, and the patterned one is the I atom. An I interstitial atom occupies the lattice of a Si or a C atom, and the Si or C atom is squeezed into a neighbor octahedral interstitial site. The arrows point out the diffusion directions. The diffusion length is the distance between the I atom and a neighbor Si or C atom along the corresponding diffusion path.

TABLE I

Migration Energy Barriers and Attempt-to-Diffuse Frequencies of an I Atom in SiC Along Paths A, B, C, and D

Path	E_d (eV)	Γ_0 (THz)
A	1.20	25.12
B1	0.88	5.02
B2	1.20	16.24
C	0.19	9.12
D1	0.19	2.14
D2	1.30	44.38
D3	0.20	2.56

is $E_C = 0.19$ eV. Decompose path D into three parts, and the diffusion barriers are $E_{D1} = 0.19$ eV, $E_{D2} = 1.30$ eV, and $E_{D3} = 0.20$ eV. The second step is the control step of path D. So, the energy barrier for path C is much lower than that of path D. Consequently, an I interstitial atom diffuses relatively more easily along path C than it diffuses along path D.

If an I interstitial atom diffuses in bulk SiC, I may travel along a series of combinations of $I_{Si} \rightarrow I_c$ and $I_c \rightarrow I_{Si}$. Because of the symmetry, an I atom can travel along eight $[\pm 1\ \pm 1\ \pm 1]$ directions. With the combination of these paths, an I interstitial can travel throughout the whole solid. Figure 3 shows a possible zigzag path with the combination of $I_{Si} \rightarrow I_c$ and $I_c \rightarrow I_{Si}$.

III.A.3. Diffusion Rates of I Atom Diffusion in Bulk SiC

For a random walk diffusion process, the frequency of diffusion follows the Arrhenius law[36]:

$$\Gamma = \Gamma_0 \exp\left(-\frac{E_A}{k_B T}\right), \tag{2}$$

where E_A is the diffusion barrier and Γ_0 is the attempt-to-diffuse frequency. For an N atom system, with transition state theory[37] and classical harmonic approximation, the frequency of a diffusion event is $\Gamma_0 = n\nu$, where n is the number of equivalent diffusion paths and ν can be written as

$$\nu = \frac{\Pi_{i=1}^{3N} \nu_i}{\Pi_{i=1}^{3N-1} \nu_i'}, \tag{3}$$

where ν_i are the $3N$ normal modes of the system at the initial state. The ν_i' are the normal modes at the saddle point. Because there is an imaginary frequency at the saddle point, the product in the denominator contains only $3N - 1$ frequencies.

The attempt-to-diffuse frequencies of the four diffusion paths are calculated in this section. Coupled with the diffusion energy barriers, the frequencies of the diffusion events are plotted as a function of temperature (see Fig. 5). The attempt-to-diffuse frequencies are listed in Table I.

The frequencies of the diffusion as a function of temperature in the range of 300 to 3000 K are shown in Fig. 5. In path B, the diffusion rate of B1 is higher than the rate of B2. Step B2 is the control step of path B. The diffusion rate of path A is higher than that of B2 (see Fig. 5a). Therefore, an I interstitial will diffuse more likely from a Si lattice site to a C lattice site via path A.

In multiple diffusion path D, the diffusion rate of step D2 is lower than the rates of steps D1 and D3 (see Fig.

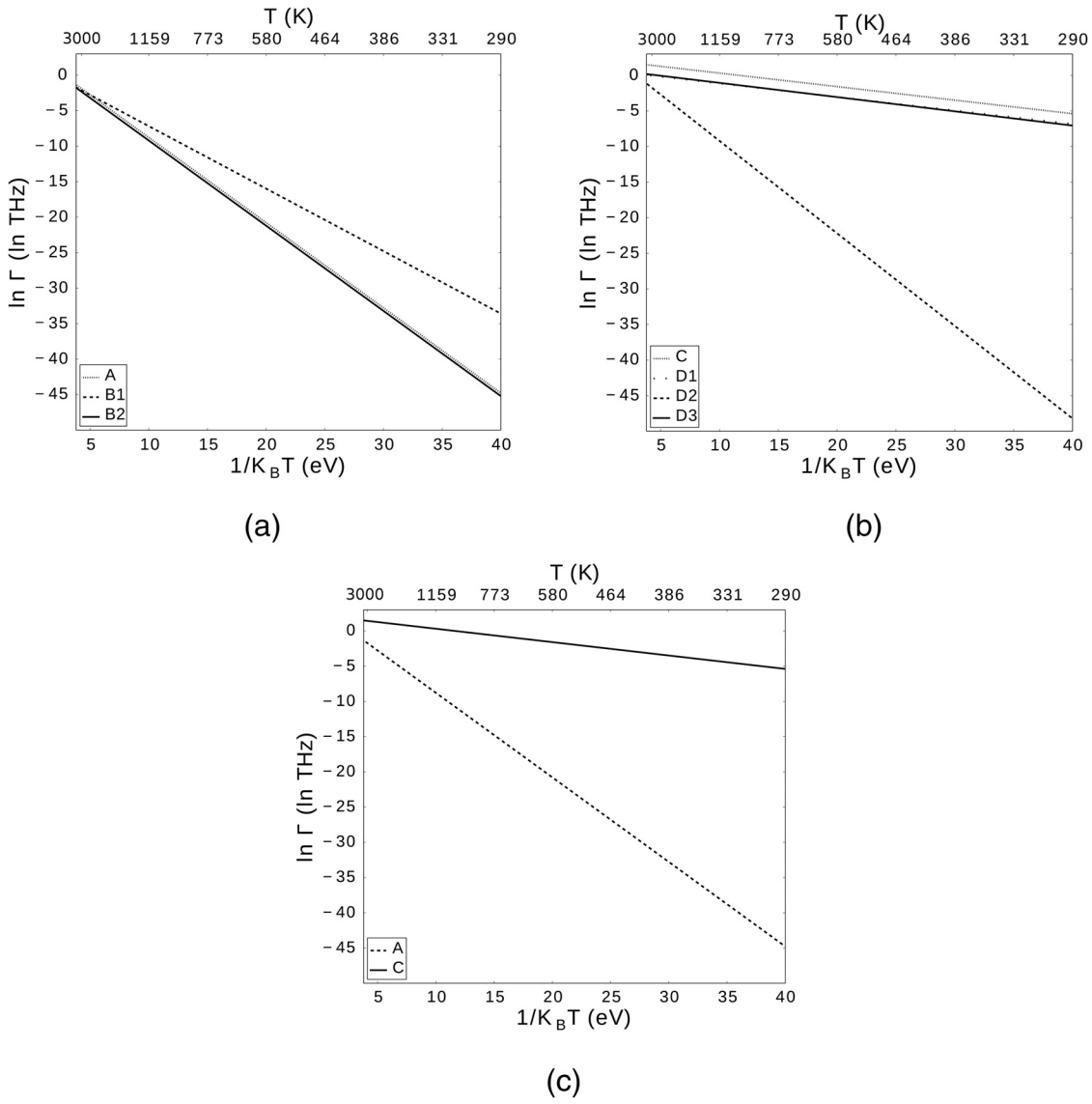

Fig. 5. The diffusion rate of I diffusion in SiC as a function of temperature in the range of 300 to 3000 K. (a) The diffusion rates of paths A and B; diffusion along path A is faster than path B. (b) The diffusion rates of paths C and D; diffusion along path C is faster. (c) The diffusion rates of paths A and C. The diffusion rate of path A is lower, and it is the control step of I diffusion in SiC.

5b). Step D2 is the control step of path D. The diffusion rate of path C is higher than the rate of step D2 (see Fig. 5b). Therefore, path C is the preferred path for I interstitial atom diffusion from a C lattice site to a Si lattice site. The diffusion frequency of step A is much lower than the frequency of path C (see Fig. 5c). As we mentioned before, I interstitial atom diffusion in bulk SiC via a multiple step path is a combination of $I_{Si} \rightarrow I_c$ and $I_c \rightarrow I_{Si}$. Therefore, path A is the control step of I interstitial diffusion in solid SiC. As a result, the diffusion frequency of path A represents the frequency of iodine diffusion in SiC. The diffusion barrier of I interstitial diffusion in solid SiC is 1.20 eV, and the attempt-to-diffuse frequency is 25.12 THz.

III.B. Iodine Interstitial Diffusion in Bulk Zr

III.B.1. Configurations of an I Interstitial Atom in Bulk Zr

Hexagonal close packed α-Zr is composed of hexagonal atom layers as the ABAB . . . sequence along the [0001] direction (see Fig. 6). Our calculated lattice parameters of α-Zr crystal are $a = 3.235$ Å and $c = 5.159$ Å, which is close to the experimental data of $a = 3.231$ Å and $c = 5.148$ Å (Ref. 38). They also agree with lattice parameters from theoretical calculation with a similar method, which are $a = 3.2276$ Å and $c = 5.1516$ Å (Ref. 39). With these calculated lattice parameters, a

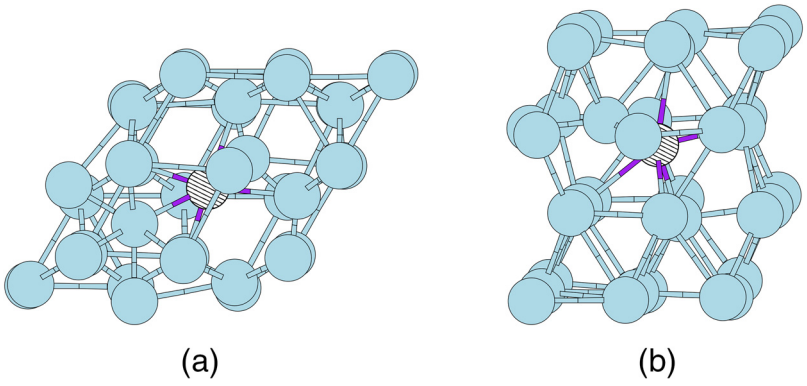

Fig. 6. The configuration of an I interstitial atom in bulk Zr. (a) Top view of the configuration and (b) side view of the supercell. The filled circles represent Zr atoms. The patterned one is the I interstitial atom that pushes a neighbor Zr atom into an interstitial site.

zirconium slab is constructed for the diffusion calculations. Because of the symmetry of the hcp structure of Zr, there is only one type of lattice site, one type of tetrahedron, one type of octahedral, and one type of substitution. From our calculations, the most stable configuration for an I interstitial atom in bulk α-Zr is that an I atom stay close to a Zr atom and the original Zr atom is squeezed into a neighbor octahedral interstitial (Fig. 6). The formation energy for this type interstitial (in a 64+1 atom supercell) is 1.32 eV.

III.B.2. Diffusion Path of an I Interstitial Atom in Bulk Zr

Because an I interstitial is close to a Zr lattice site, the path of I interstitial diffusion can be considered as an I atom migrating from a Zr lattice to another adjacent lattice. There are two different Zr-Zr edges in the Zr crystal structure (see Fig. 7). The I interstitial atom can diffuse along these two edges, named paths E and F in Fig. 7. Path E is along the [1000] direction, and path F is along the [0001] direction in Zr bulk.

When an I interstitial diffuses along path E, the schematic of its diffusion path and corresponding energy barriers are shown in Fig. 8. The I atom diffuses between two Zr atom layers along a zigzag path. The path can be decomposed into two steps: steps E1 and E2. For step E1, an I interstitial atom diffuses from position *a* to an adjacent position *b*; the diffusion barrier is $E_{E1} = 0.16$ eV. For step E2, an I interstitial atom diffuses from position *b* to an adjacent position *c* along a Zr-Zr edge; the energy barrier is $E_{E2} = 0.14$ eV. Therefore, step E1 is the control step with a diffusion energy barrier of 0.16 eV along the [1000] direction.

Since hcp Zr is composed of ABAB . . . layers, once an I interstitial atom travels from a layer to another equivalent layer, it will go through another Zr atomic layer. As a result, diffusion path F can also be decomposed into two

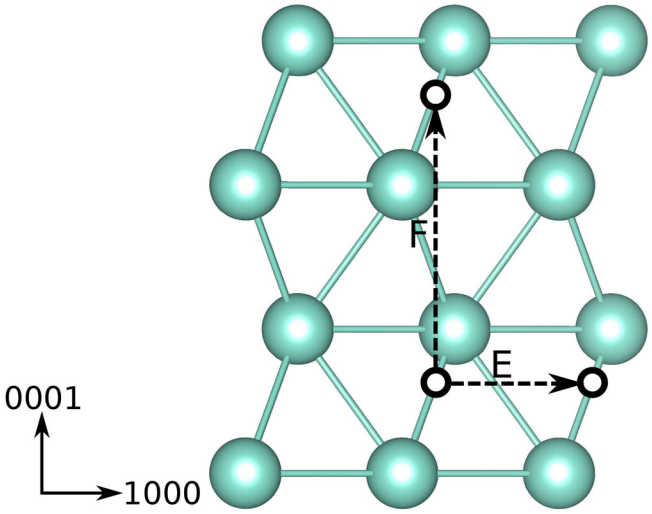

Fig. 7. Diffusion paths E and F of an iodine atom from a Zr lattice to another adjacent site. Along path E, an I atom travels between two Zr atom layers, while along path F, an I atom travels from one Zr layer to another layer. The big balls represent Zr atoms, and the small unfilled black circles represent the possible interstitial positions of an iodine atom in bulk Zr. The arrows with dotted lines point out the diffusion directions.

steps: paths F1 and F2 (Fig. 9). For step F1, the diffusion energy barrier is $E_{F1} = 0.23$ eV; an I atom goes across a Zr layer from position *a* to *b*. For step F2, the I atom diffuses along a Zr-Zr edge to an adjacent position *c* at another Zr atom layer, and the diffusion energy barrier is $E_{F2} = 0.14$ eV. Step F2 is similar to step E2, and the diffusion barriers for F2 and E2 are the same. This suggests that it is more difficult for interlayer diffusion than inner-layer diffusion. In this diffusion path, step F1 is the control step with a diffusion energy barrier of 0.23 eV along the [0001] direction. These results are consistent with the energy barrier (0.24 eV) of Rossi and Taylor's work.[18]

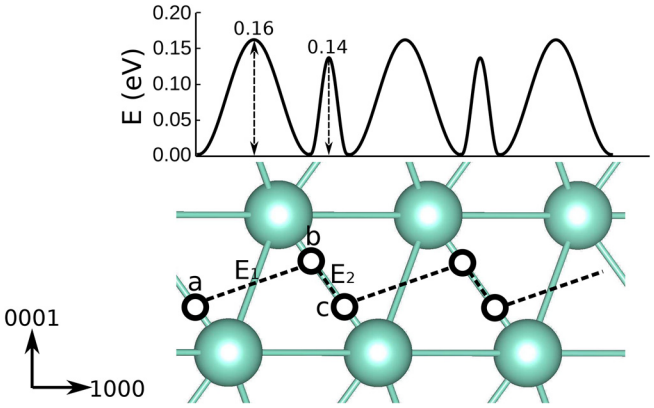

Fig. 8. An I interstitial atom diffuses along [1000] direction in Zr bulk. The upper plot is the energy profile, and the corresponding diffusion path is shown below. The big balls represent Zr atoms. The small unfilled black circles represent the positions of an iodine atom in Zr bulk along the diffusion path. The I interstitial atom diffuses along the dotted lines.

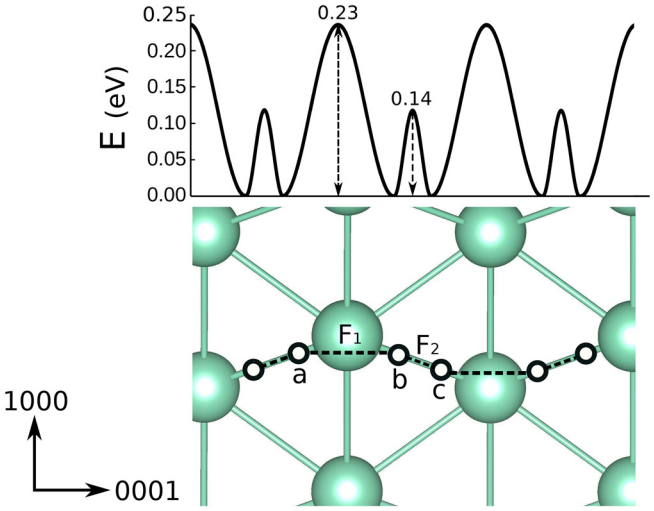

Fig. 9. An I atom diffuses across different Zr atom layers along [0001] direction. The upper plot is the energy profile along the diffusion path, and the corresponding diffusion path is shown below. The big balls represent Zr atoms. The small black unfilled circles represent the possible interstitial positions of an iodine atom along the diffusion path, which is represented by the dotted lines.

III.B.3. Diffusion Rates of I Atom Diffusion in Bulk Zr

The attempt-to-diffuse frequencies of the two diffusion paths are calculated in this section. Plugging the diffusion energy barriers and the attempt-to-diffuse frequencies into Eq. (2), the diffusion rates of I atom diffusion in bulk Zr are plotted as a function of temperature (see Fig. 10). The diffusion barriers and the attempt-to-diffuse frequencies Γ_0 are listed in Table II. The diffusion rates of I atom diffusion in Zr along the [1000] direction are plotted as a function of temperature in Fig. 10a. An intersection point appears at 610.6 K. When the temperature is <610.6 K, step E1 is the control step. If the temperature is >610.6 K, step E2 is the control step.

With Eq. (2) and the data in Table II, the diffusion rates of I atom diffusion across atom layers along the [0001] direction in bulk Zr are plotted as a function of temperature in Fig. 10b. In the temperature range from 290 to 3000 K, the diffusion rate of an I atom in Zr via step F1 is much lower than that via step F2. Therefore, F1 is the control step of this diffusion process.

The diffusion rates of I atom diffusion across a Zr atom layer and along a Zr atom layer are plotted in Fig. 10c. In the temperature range from 290 to 3000 K, the interlayer diffusion rate is slower than the inner-layer diffusion rate. Therefore, an I atom would prefer to diffuse in bulk α-Zr between two layers along a zigzag path rather than to diffuse across two Zr atom layers in the [0001] direction. When the temperature is <610.6 K, the energy barrier is 0.16 eV, and the diffusion frequency is 2.88 THz. When the temperature is >610.6 K, the energy barrier is 0.14 eV, and the diffusion frequency is 1.97 THz.

For hcp Zr, the [1000] and [0100] directions are equivalent. Therefore, with the combination of the diffusion in these two directions, an I atom could travel two-dimensionally along a zigzag path.

III.C. Compare I Atom Diffusion in Bulk SiC and Zr

III.C.1. Formation Energies of an I Interstitial Atom in Bulk SiC and Zr

The formation energies of an I interstitial atom in bulk SiC and Zr are calculated and listed in Table III. E_{Pure} represents the system energy of a SiC or a Zr supercell without any I atom. E_i represents the total energy of a SiC or a Zr supercell with an I interstitial atom. E_I is the ground state energy of an iodine atom in an empty box the same as the box of a SiC or a Zr supercell. Because the box for a SiC supercell is different from the box for a Zr supercell, the energies for an I atom are different for the two boxes.

The formation energy of an I interstitial in Zr is 1.32 eV. The active energy including the formation energy and the diffusion energy barrier is 1.48 eV. This value is consistent with the experimental result of 1.7 eV (Ref. 13). The formation energy for an I interstitial in a SiC supercell is about ten times higher than the formation energy of an I interstitial in a Zr supercell. Both formation energies are positive, and this indicates the systems need to adsorb thermal energies to introduce an I interstitial. The formation

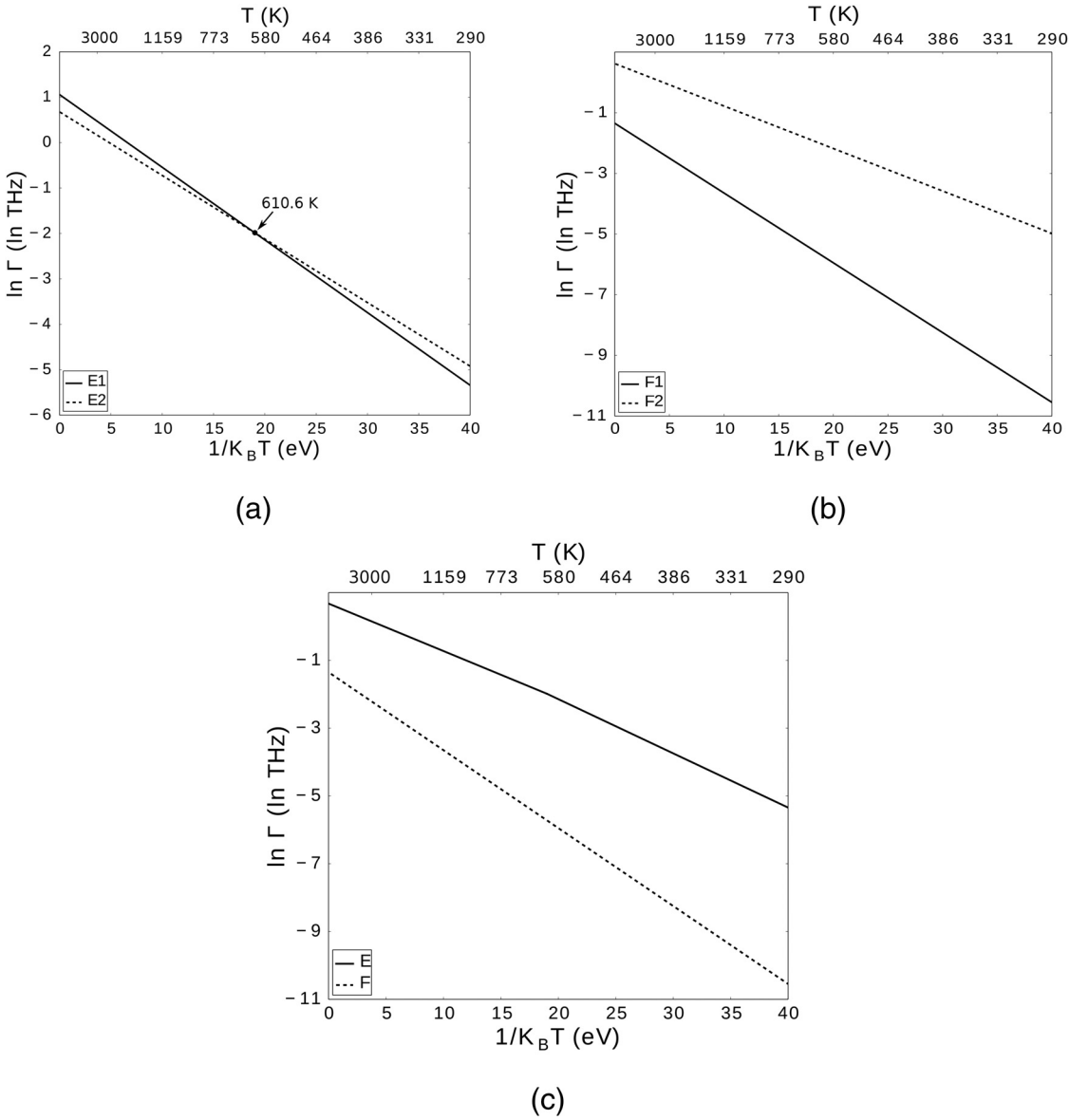

Fig. 10. Diffusion rates of I atom diffusion in bulk Zr. (a) Paths E1 and E2: An I atom diffusion along [1000] direction (path E). Step E1 is the control step when temperature is <610.6 K. Step E2 is the control step if the temperature is >610.6 K. (b) Paths F1 and F2: An I atom diffusion along [0001] direction (path F). Step F1 is the control process. (c) Paths E and F1: Diffusion rates of an I atom along paths E and F. An I atom diffusion along a Zr layer (E1 + E2) is faster than the diffusion between different atom layers (path F).

TABLE II

Diffusion Barriers and Attempt-To-Diffuse Frequencies for I Atom Diffusion Along Paths E and F

Path	E_d (eV)	Γ_0 (THz)
E1	0.16	2.88
E2	0.14	1.97
F1	0.23	0.26
F2	0.14	1.86

TABLE III

Formation Energies E_i^f of an I Interstitial Atom in SiC and Zr*

	E_{pure} (eV)	E_1 (eV)	E_i (eV)	E_i^f (eV)
SiC	−481.97	−0.20	−467.76	14.41
Zr	−542.60	−0.20	−541.48	1.32

*E_{pure} = total energy of a SiC or a Zr supercell without any iodine atom; E_i = total energy of a SiC or a Zr supercell with an iodine interstitial atom; E_1 = ground state energy of an iodine atom in an empty box for a SiC or a Zr supercell.

energies show that it is more difficult to form an I interstitial defect in bulk SiC than that in bulk Zr. The atomic radius of an I atom (1.40 Å) is much larger than that of a Si atom (1.20 Å) or a C atom (0.68 Å), but it is close to that of a Zr atom (1.55 Å) (Ref. 40). The radius difference may make the formation energy in SiC very high.

III.C.2. Diffusion Path of I Interstitial Atom Diffusion in Bulk SiC and Zr

The dominant diffusion mechanism of an I interstitial atom traveling in bulk SiC or Zr is the exchange mechanism. An I atom pushes a Si, a C, or a Zr atom out of its lattice to an interstitial site and takes its position. Once the I atom diffuses ahead, it will take the lattice position of another atom and generate another interstitial atom. Generally, the diffusion process happens along a Si-C or a Zr-Zr bond. Although an I atom may diffuse along different directions, the diffusion rates in different directions are roughly the same in SiC. As a result, the diffusion of an I interstitial atom in bulk SiC is almost an isotropic process. Hexagonal close packed Zr crystal can be decomposed into hexagonal atom layers along the [0001] direction. It is relatively more difficult for an I atom traveling across different layers. An I interstitial atom prefers to travel along a (0001) plane. So, the diffusion in bulk Zr is an anisotropy process.

III.C.3. Diffusion Rates of I Interstitial Atom Diffusion in Bulk SiC and Zr

The diffusion rates of an I interstitial atom in bulk SiC and Zr are plotted as a function of temperature in Fig. 11. The diffusion rate of an I atom in bulk SiC is much lower than that of an I atom in bulk Zr in the temperature range considered. Therefore, iodine diffusion via the interstitial site in SiC is slower than that in Zr. Because of the exsistence of point defect, grain boundary, dislocation, and stacking fault, an I atom may diffuse faster at those defects. It is of interest to study the defect effect on the diffusion behavior in the future.

IV. CONCLUSIONS

Using first-principles calculations and the NEB method, the metastable configurations of an I interstitial in bulk β-SiC and α-Zr are determined, and the diffusion mechanisms of an I interstitial in SiC and Zr have been investigated. The formation energy of an I interstitial atom in bulk SiC is ten times larger than that of an I atom in bulk Zr. The I interstitial is very difficult to introduce into SiC compared with the doping process of an I atom in bulk Zr. The diffusion mechanism of an I interstitial in SiC and Zr is the exchange mechanism. Iodine diffusion in the bulk SiC is roughly isotropic. It is a multistep diffusion process along a path that is a series of combinations of $I_{Si} \rightarrow I_c$ and $I_c \rightarrow I_{Si}$, with a diffusion barrier of 1.20 eV and an attempt-to-diffuse frequency $\Gamma_0 = 25.12$ THz. Iodine atom diffusion in bulk Zr is an anisotropic process. An I interstitial atom diffuses mainly between two Zr atom (0001) layers along a zigzag path with a diffusion barrier of 0.16 eV and an attempt-to-diffuse frequency $\Gamma_0 = 2.88$ THz. Interlayer diffusion is relatively difficult. In general, the diffusion rate of an I interstitial in bulk SiC is lower than that in bulk Zr in the temperature range from 290 to 3000 K.

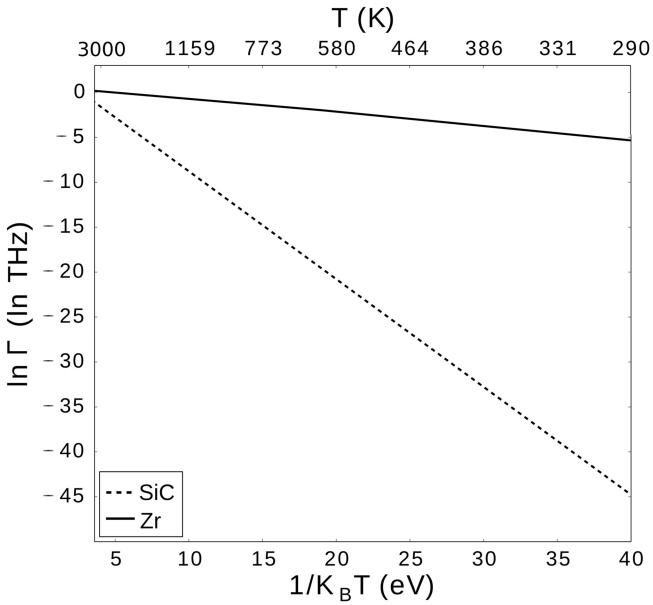

Fig. 11. Diffusion rates as a function of temperature for I interstitial atom diffusion in bulk SiC and Zr. Diffusion in SiC is slower than that in Zr in the temperature range considered.

Acknowledgments

This work is supported by the Essential Research Fund of State Nuclear Power Technology Company, China (SNPTC). The SNPTC support is under contract 2013SN010-001. It is also supported by National Science and Technology Major Project of China under contracts 2013ZX06004007-006 and 2015ZX06004001-002.

References

1. C. AZEVEDO, "Selection of Fuel Cladding Material for Nuclear Fission Reactors," *Eng. Fail. Anal.*, **18**, *8*, 1943 (2011); http://dx.doi.org/10.1016/j.engfailanal.2011.06.010.

2. J. B. MALHERBE, "Diffusion of Fission Products and Radiation Damage in SiC," *J. Phys. D Appl. Phys.*, **46**, *47*, 473001 (2013); http://dx.doi.org/10.1088/0022-3727/46/47/473001.
3. C. LEMAIGNAN and A. T. MOTTA, "Zirconium Alloys in Nuclear Applications," *Materials Science and Technology*, Wiley-VCH Verlag GmbH and Company (2006).
4. P. ZHOU et al., "Electronic and Optical Properties of Co-Doped 3C-SiC from Density Functional Calculations," *Solid State Commun.*, **196**, 28 (2014); http://dx.doi.org/10.1016/j.ssc.2013.10.024.
5. J. DU, B. WEN, and R. MELNIK, "Mechanism of Hydrogen Production via Water Splitting on 3C-SiCs Different Surfaces: A First-Principles Study," *Comput. Mater. Sci.*, **95**, 451 (2014); http://dx.doi.org/10.1016/j.commatsci.2014.08.018.
6. H. LATHA, A. UDAYAKUMAR, and V. S. PRASAD, "Microstructure and Electrical Properties of Nitrogen Doped 3C-SiC Thin Films Deposited Using Methyltrichlorosilane," *Mater. Sci. Semicond. Process.*, **29**, 117 (2015); http://dx.doi.org/10.1016/j.mssp.2013.12.017.
7. Q. WANG et al., "Molecular Dynamics Study on Interfacial Thermal Conductance of Unirradiated and Irradiated SiC/C," *Nucl. Instrum. Methods Phys. Res. B*, **328**, 42 (2014); http://dx.doi.org/10.1016/j.nimb.2014.03.004.
8. C.-Y. HO et al., "Microstructural Investigation of Si-Ion-Irradiated Single Crystal 3C-SiC and SA-Tyrannohex SiC Fiber-Bonded Composite at High Temperatures," *J. Nucl. Mater.*, **443**, *1–3*, 1 (2013); http://dx.doi.org/10.1016/j.jnucmat.2013.06.045.
9. E. FRIEDLAND et al., "Study of Iodine Diffusion in Silicon Carbide," *Nucl. Instrum. Methods Phys. Res. B*, **268**, *19*, 2892 (2010); http://dx.doi.org/10.1016/j.nimb.2010.04.015.
10. P. SIDKY, "Iodine Stress Corrosion Cracking of Zircaloy Reactor Cladding: Iodine Chemistry (A Review)," *J. Nucl. Mater.*, **256**, *1*, 1 (1998); http://dx.doi.org/10.1016/S0022-3115(98)00044-0.
11. B. LEWIS et al., "Modelling of Iodine-Induced Stress Corrosion Cracking in CANDU Fuel," *J. Nucl. Mater.*, **408**, *3*, 209 (2011); http://dx.doi.org/10.1016/j.jnucmat.2010.10.063.
12. J. KALILAINEN et al., "Chemical Reactions of Fission Product Deposits and Iodine Transport in Primary Circuit Conditions," *Nucl. Eng. Des.*, **267**, 140 (2014); http://dx.doi.org/10.1016/j.nucengdes.2013.11.078.
13. N. MONCOFFRE, G. CARLOT, and A. CHEVARIER, "Diffusion Study of Implanted Iodine in Zirconium Using Ion Beams," *Surf. Coat. Technol.*, **128**, 9 (2000); http://dx.doi.org/10.1016/S0257-8972(00)00636-8.
14. A. AUDREN et al., "Ion Implantation of Iodine into Silicon Carbide: Influence of Temperature on the Produced Damage and on the Diffusion Behaviour," *Nucl. Instrum. Methods Phys. Res. B*, **266**, *12*, 2810 (2008); http://dx.doi.org/10.1016/j.nimb.2008.03.123.
15. E. FRIEDLAND et al., "Investigation of Silver and Iodine Transport Through Silicon Carbide Layers Prepared for Nuclear Fuel Element Cladding," *J. Nucl. Mater.*, **410**, *1*, 24 (2011); http://dx.doi.org/10.1016/j.jnucmat.2010.12.243.
16. P. HOHENBERG and W. KOHN, "Inhomogeneous Electron Gas," *Phys. Rev.*, **136**, B864 (1964); http://dx.doi.org/10.1103/PhysRev.136.B864.
17. E. WIMMER et al., "*Ab Initio* Calculations for Industrial Materials Engineering: Successes and Challenges," *J. Phys. Condens. Matter*, **22**, *38*, 384215 (2010); http://dx.doi.org/10.1088/0953-8984/22/38/384215.
18. M. L. ROSSI and C. D. TAYLOR, "First-Principles Insights into the Nature of Zirconium–Iodine Interactions and the Initiation of Iodine-Induced Stress–Corrosion Cracking," *J. Nucl. Mater.*, **458**, 1 (2015); http://dx.doi.org/10.1016/j.jnucmat.2014.11.114.
19. D. SHRADER, I. SZLUFARSKA, and D. MORGAN, "Cs Diffusion in Cubic Silicon Carbide," *J. Nucl. Mater.*, **421**, *1*, 89 (2012); http://dx.doi.org/10.1016/j.jnucmat.2011.11.051.
20. D. SHRADER et al., "Ag Diffusion in Cubic Silicon Carbide," *J. Nucl. Mater.*, **408**, *3*, 257 (2011); http://dx.doi.org/10.1016/j.jnucmat.2010.10.088.
21. R. RURALI et al., "First-Principles Studies of the Diffusion of B Impurities and Vacancies in SiC," *Phys. Rev. B*, **69**, *12*, 125203 (2004); http://dx.doi.org/10.1103/PhysRevB.69.125203.
22. W. KOHN and L. J. SHAM, "Self-Consistent Equations Including Exchange and Correlation Effects," *Phys. Rev.*, **140**, A1133 (1965); http://dx.doi.org/10.1103/PhysRev.140.A1133.
23. G. KRESSE and J. HAFNER, "*Ab Initio* Molecular Dynamics for Liquid Metals," *Phys. Rev. B*, **47**, 558 (1993); http://dx.doi.org/10.1103/PhysRevB.47.558.
24. G. KRESSE and J. HAFNER, "*Ab Initio* Molecular-Dynamics Simulation of the Liquid-Metal–Amorphous-Semiconductor Transition in Germanium," *Phys. Rev. B*, **49**, 14251 (1994); http://dx.doi.org/10.1103/PhysRevB.49.14251.
25. P. E. BLÖCHL, "Projector Augmented-Wave Method," *Phys. Rev. B*, **50**, 17953 (1994); http://dx.doi.org/10.1103/PhysRevB.50.17953.
26. G. KRESSE and D. JOUBERT, "From Ultrasoft Pseudopotentials to the Projector Augmented-Wave Method," *Phys. Rev. B*, **59**, 1758 (1999); http://dx.doi.org/10.1103/PhysRevB.59.1758.
27. J. P. PERDEW, K. BURKE, and M. ERNZERHOF, "Generalized Gradient Approximation Made Simple," *Phys. Rev. Lett.*, **77**, 3865 (1996); http://dx.doi.org/10.1103/PhysRevLett.77.3865.

28. J. P. PERDEW, K. BURKE, and M. ERNZERHOF, "Generalized Gradient Approximation Made Simple [Phys. Rev. Lett., 77, 3865 (1996)]," *Phys. Rev. Lett.*, **78**, 1396 (1997); http://dx.doi.org/10.1103/PhysRevLett.78.1396.

29. G. KRESSE and J. FURTHMÜLLER, "Efficiency of Ab-Initio Total Energy Calculations for Metals and Semiconductors Using a Plane-Wave Basis Set," *Comput. Mater. Sci.*, **6**, 15 (1996); http://dx.doi.org/10.1016/0927-0256(96)00008-0.

30. G. KRESSE and J. FURTHMÜLLER, "Efficient Iterative Schemes for *Ab Initio* Total-Energy Calculations Using a Plane-Wave Basis Set," *Phys. Rev. B*, **54**, 11169 (1996); http://dx.doi.org/10.1103/PhysRevB.54.11169.

31. H. JÓNSSON, G. MILLS, and K. W. JACOBSEN, "Chapter 16: Nudged Elastic Band Method for Finding Minimum Energy Paths of Transitions," *Classical and Quantum Dynamics in Condensed Phase Simulations*, B. J. BERNE, G. CICCOTTI, and D. F. COKER, Eds., p. 385, World Scientific (1998).

32. G. HENKELMAN and H. JÓNSSON, "Improved Tangent Estimate in the Nudged Elastic Band Method for Finding Minimum Energy Paths and Saddle Points," *J. Chem. Phys.*, **113**, 9978 (2000); http://dx.doi.org/10.1063/1.1323224.

33. G. HENKELMAN, B. P. UBERUAGA, and H. JÓNSSON, "A Climbing Image Nudged Elastic Band Method for Finding Saddle Points and Minimum Energy Paths," *J. Chem. Phys.*, **113**, 9901 (2000); http://dx.doi.org/10.1063/1.1329672.

34. "Transition State Tools for VASP" (2014); http://theory.cm.utexas.edu/vtsttools/download.html (current as of Aug. 12, 2015).

35. "Silicon Carbide (SiC), Lattice Parameters, Thermal Expansion," in "Group IV Elements, IV–IV and III–V Compounds. Part b—Electronic, Transport, Optical and Other Properties," *Landolt-Börnstein–Group III Condensed Matter*, O. MADELUNG, U. RÖSSLER, and M. SCHULZ, Eds., Vol. 41A1b, pp. 1–11, Springer (2002).

36. G. BOISVERT and L. J. LEWIS, "Self-Diffusion on Low-Index Metallic Surfaces: Ag and Au (100) and (111)," *Phys. Rev. B*, **54**, 2880 (1996); http://dx.doi.org/10.1103/PhysRevB.54.2880.

37. G. H. VINEYARD, "Frequency Factors and Isotope Effects in Solid State Rate Processes," *J. Phys. Chem. Solids*, **3**, *1–2*, 121 (1957); http://dx.doi.org/10.1016/0022-3697(57)90059-8.

38. B. OLINGER and J. C. JAMIESON, "Zirconium: Phases and Compressibility to 120 Kilobars," *High Temp. High Press.*, **5**, 123 (1973).

39. M. V. GLAZOFF et al., "Oxidation and Hydrogen Uptake in Zirconium, Zircaloy-2 and Zircaloy-4: Computational Thermodynamics and *Ab Initio* Calculations," *J. Nucl. Mater.*, **444**, *1–3*, 65 (2014); http://dx.doi.org/10.1016/j.jnucmat.2013.09.038.

40. W. M. HAYNES, *CRC Handbook of Chemistry and Physics*, CRC Press (2014).